4ICEGE Thessaloniki-GREECE 2007

4th International Conference on
Earthquake Geotechnical Engineering
June 25-28, 2007
Paper No.1247

OBSERVATION OF SOIL DISPLACEMENTS AROUND TUNNELS SUBJECTED TO EARTHQUAKE LOADING

Ulas Cilingir [1], S.P. Gopal Madabhushi[2]

ABSTRACT

Safety of underground structures is quite important during and following a major earthquake event. Current understanding of the seismic behavior of tunnels is rather limited and relies on elastic behavior of soil and tunnel structures. In this paper results from a series of small scale shaking table tests on physical models of tunnels embedded in shallow sand layers are presented. Square and circular tunnel sections were subjected to cyclic loading and the deformation in the tunnel section as well as in the surrounding soil is monitored using high speed digital video imaging. Deformation patterns were obtained by using Particle Image Velocimetry technique. The initial results indicate that the circular tunnel section suffer damage due to accumulated strains while square tunnel sections suffer damage due to "caving-in" of side walls of the tunnel.

Keywords: Underground structures, Seismic loading, Particle Image Velocimetry, Soil-structure interaction

INTRODUCTION

The increasing demand to underground transportation facilities in earthquake prone areas, especially in developing countries, raised some issues regarding the safety of the underground structures against earthquakes. Recent events such as Kobe Earthquake in Japan (1995), Duzce Earthquake in Turkey (1999), Chi-chi Earthquake in Taiwan (1999) and Bam Earthquake in Iran (2003) showed that the poor seismic design of these facilities may cost both lives and money. Our understanding of failure mechanisms of underground structures subjected to an earthquake event is limited. Also the lack of observational data prevents us to use reliable empirical relationships.

Case studies reveal that the depth of the tunnel below the ground surface, the type of soil or rock surrounding the tunnel, the maximum ground acceleration, the intensity of the earthquake, the distance to the earthquake epicenter and the type of tunnel lining affect the behavior of the tunnels under earthquake loading. Underground structures are reported to suffer less damage than the surface structures and the reported damage decreases with overburden depth. Also the duration of the earthquake is crucial, because the long earthquakes with many load cycles may cause fatigue damage in linings. Case studies also showed that the accelerations amplified upon incidence onto a tunnel, if the wavelengths are between one and four times the tunnel diameter. Damage may be related to the peak ground acceleration and velocity or fault movements. The slope-stability at or near tunnel portals may cause significant damage. Floatation and sinking of the tunnel due to liquefaction are also reported to be main sources of damage in the tunnels (Hashash et al., 2001; Wang et al., 2001 and Pakbaz and Yareevand, 2005).

[1] Ph.D. Student, Department of Engineering, University of Cambridge, UK, Email: uc206@cam.ac.uk
[2] Reader, Department of Engineering, University of Cambridge, UK

Current design methods include analytical methods based on elasticity theory which ignore the effects of inertia. Free-field approach, which is the simplest method of analysis, assumes that the strains in the tunnel structure to be the same as the free-field strains (St. John and Zahrah, 1987). Other methods use strain compatibility functions to find the effect of soil lining on the ground deformations (Wang, 1993; Penzien and Wu, 1998; Penzien, 2000; Hashash et al., 2001, Bobet et al., 2006). A pseudostatic pure shear load is applied on the soil around the tunnel and elastic stress distribution functions are used to find the strains. The superposition of deformations in the lining and on the walls of a cylindrical cavity is used to find the stresses in the tunnel lining as a function of the flexibility ratio, which is a commonly used to measure the flexural stiffness of the medium relative to the tunnel lining. It should be noted that both the ground and the tunnel lining are assumed to be elastic. Daikai station of the Kobe subway system, which was designed using above methodology, has collapsed in 1995 Kobe earthquake (Huo, 2005).

Dynamic earth pressure models like the commonly used Mononobe-Okabe method developed for retaining walls are also used in the case of shallow rectangular tunnels. Hashash et al. (2001) state that the accuracy of these methods decreases with increasing tunnel embedment.

Dynamic soil-structure interaction analysis of tunnels is complex if the inelasticity, damping and inertial effects are considered. Numerical methods are commonly used to cope with this problem, but the results can only be reliable if there is no uncertainty in the input and the method. Unfortunately, there is little experimental data and few case studies to validate the use of numerical methods. Esmaeili et al. (2006) reports a number of numerical analyses conducted since 1960's. The methods include different wave function expansions, different tunnel geometries and different soil-structure interaction models.

In this paper, the emphasis will be on the dynamic soil-structure interaction between the tunnel and the surrounding soil. Small scale shaking-table tests were conducted on flexible tunnel sections with different geometries and overburden pressures in dry, soft sand. The deformation field around the tunnel was measured using Particle Image Velocimetry (PIV) technique. The aim of the experiments was to obtain an insight of the failure mechanisms experienced during strong earthquake motions under low confinement conditions.

EXPERIMENTAL SETUP

Shaking Table and the Model Box

The shaking table used in the experiments stores angular momentum by means of a rotating flywheel (See figure 1) and a mechanical clutch releases the energy stored in the flywheel after reaching the threshold. A crank mechanism converts the rotation to horizontal shaking. The crank's offset can be adjusted between 0-11mm to give the desired amplitude to the sinusoidal motion. The speed of the flywheel can also be adjusted to have a desired input motion frequency from 0 up to around 4.9 Hz. It is possible to obtain peak accelerations up to 1.4 g. This simple shaking table was used to investigate several earthquake related problems before (Marketos and Madabhushi, 2004; Knappett et al., 2005).

The model was prepared inside a wooden model box which has internal dimensions of 700mm long by 300mm wide and 500mm deep as shown in figure 1. The box has a perspex viewing window which enables the deformations of the tunnel structure and of the soil around the tunnel to be observed. Control markers drawn on the perspex window makes it possible to measure the rigid body motion experienced by the model during the shaking. It is also used for the image calibration in PIV analyses.

Model Tunnels

The model tunnels are made of 0.25mm thick aluminum. Circular tunnels have a diameter of 100 mm and the square tunnels have a width of 90mm. The embedment depths vary from 90mm to 100mm as shown in the figure 2. All tunnel sections have a length of 295mm.

For circular tunnels, the flexural stiffness of the medium relative to the tunnel lining is given by the flexibility ratio F, which is expressed as (Merritt et al., 1985):

$$F = \frac{E_m\left(1-\upsilon_l{}^2\right)R^3}{6E_l I(1+\upsilon_m)} \tag{1}$$

where E_m is the modulus of elasticity of the medium, E_l is the modulus of elasticity of the tunnel lining, I is the moment of inertia of the lining (per unit width) for circular tunnel having a radius R, υ_m is the Poisson's ratio of the medium and υ_l is the Poisson's ratio of the lining. The initial modulus of elasticity of the medium can be found using the empirical relationship given by Hardin and Drnevich (1972) for small-strain shear modulus as shown in equation 2.

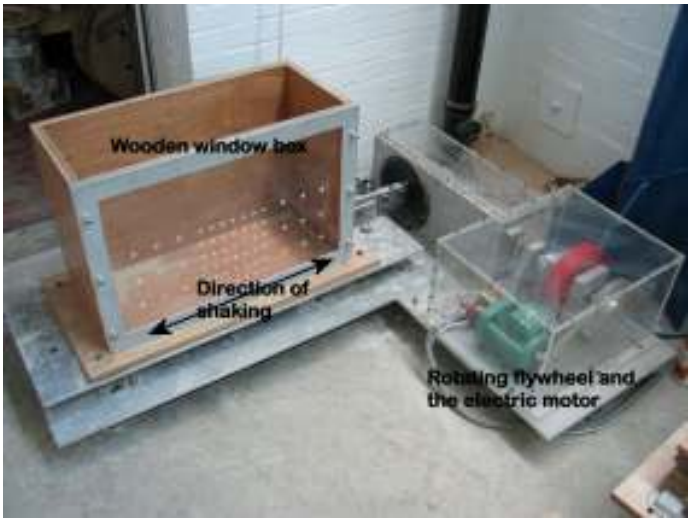

Figure 1. Shaking Table

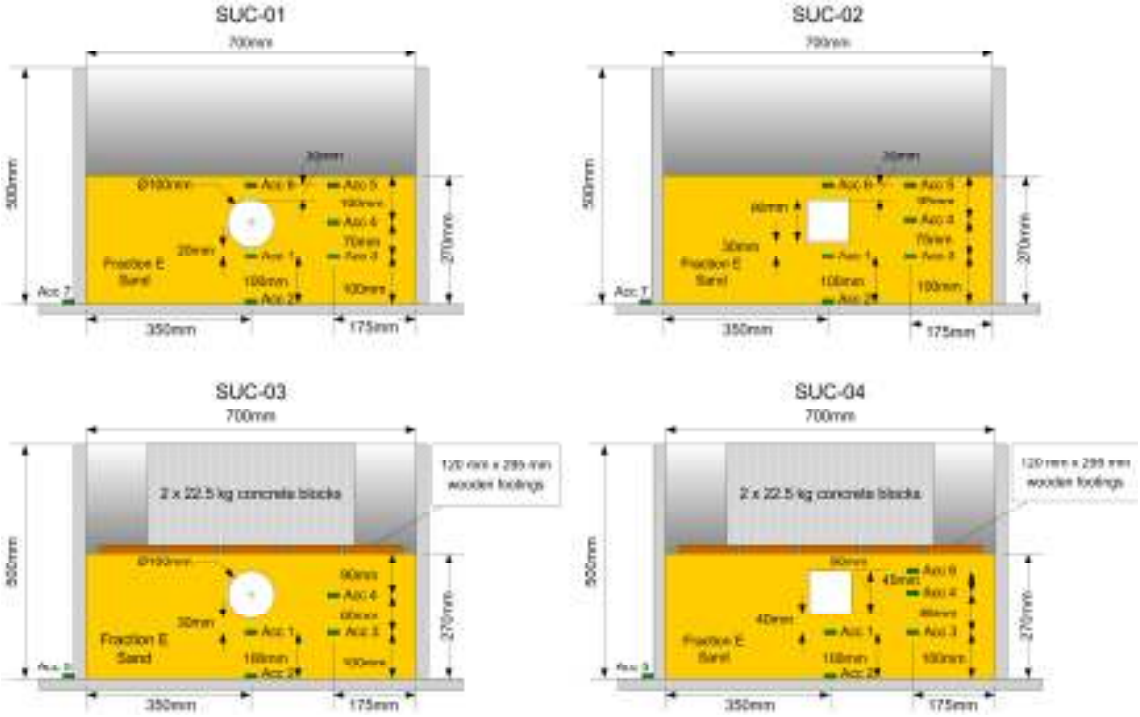

Figure 2. Layout of Experiments

$$G_{\max} = 100\frac{(3-e)^2}{(1+e)}(p')^{0.5} \quad (2)$$

The modulus of elasticity can then be found using the following relationship:

$$E_m = 2G_{\max}(1+\upsilon_m) \quad (3)$$

The flexibility ratio for a rectangular tunnel can be found using following relationship (Wang, 1993):

$$F = \frac{G_m W}{S_1 H} \quad (4)$$

where S_1 is the unit racking stiffness per unit width found by simple frame analysis, W is the width of the structure, H is the height of the tunnel and G_m is the shear modulus of the medium which can be found using equation 2.

If we take the Poisson's ratio of the sand as 0.3, the flexibility ratio of the lining relative to the surrounding soil becomes 3187 and 2521.21 for circular and square tunnels respectively. These values show that the tunnel structure is much more flexible than the surrounding soil although the estimated shear modulus of the soil medium is very small due to the low mean effective confining pressure.

Instrumentation

Miniature accelerometers were used to measure accelerations at several points in the model. Images were captured for PIV analyses using the Photonics Phantom Camera. The camera is capable of taking a thousand 1024x1024 grayscale images per second. It has an internal memory of 1000 frames. In this set of tests, the pictures were taken at a rate of 80 frames per seconds which allows us to capture earthquakes up to 12.5 seconds long.

Particle Image Velocimetry (PIV) Technique

Particle Image Velocimetry (PIV) technique is a powerful tool to obtain deformation data from images taken in an experiment. It was originally developed for fluid mechanics experiments. White (2002) adopted it for use in geotechnical applications.

The basic principle of PIV analysis is to separate the image into small patches and trying to find the locations of the individual patches in consecutive images. The brightness values in the image matrix, which ranges from 0 to 256, are used to search for the most probable place of the patch in the next image by using a correlation function. The size of the patch and the search zone is determined by the user. This process is repeated for each patch and for every image in the sequence and a deformation field is obtained for the test series.

Model Preparation and Test Series

Four sets of shaking table tests on dry, loose sand were conducted. A total of 15 earthquakes were fired. The maximum input accelerations and the dominant frequencies of the earthquakes are given in table 1.

The sand pouring was done using air-pluviation method. Fraction E sand was used, which has the properties listed in table 2. Layers of dyed sand were poured in front of the perspex window to obtain extra texture for PIV images. A strip of sponge was glued around the edges of the tunnel sections to prevent sand grains to enter between the tunnel face and the perspex window. Ideally, there should be no friction between the tunnel face and the sides of the box in order to have plane strain conditions.

Therefore, a thin layer of vaseline was applied on the sponge and on the Perspex window to make sure that the tunnel slips on the perspex window.

In the tests SUC-01 and SUC-02 there was no surcharge applied on the soil surface. But, in tests SUC-03 and SUC-04 two concrete blocks of 22.5 kg were put on the surface of the soil, which applied an overburden pressure of 2.45 kPa. In these two tests, there are no accelerometers put close to the soil surface to prevent accelerometers to get damage from concrete blocks.

The camera is triggered to capture the images at a rate of 80 frames per second concurrent with the earthquake. The duration of each earthquake was approximately 10 seconds. The images stored in the internal memory of the camera were transferred to a PC hard disk after the experiment.

Table 1. Input motion characteristics for the shaking table tests

Test Set	Test Name	Maximum Input Acceleration (g)	Dominant Frequency (Hz)
SUC-01	Test 1	0.10	2.30
	Test 2	0.28	3.13
	Test 3	0.50	4.19
	Test 4	0.15	2.11
	Test 5	0.38	3.06
	Test 6	0.73	4.13
	Test 7	1.37	4.91
SUC-02	Test 1	0.25	3.08
	Test 2	0.76	4.11
	Test 3	1.39	4.96
SUC-03	Test 1	0.27	3.18
	Test 2	0.87	4.13
	Test 3	1.37	4.91
SUC-04	Test 1	0.26	3.13
	Test 2	1.13	4.31

Table 2. Properties of Fraction E sand (Tan, 1990)

D_{10} grain size	0.095 mm
D_{50} grain size	0.14 mm
D_{60} grain size	0.15 mm
Specific Gravity G_s	2.65
Minimum Void Ratio e_{min}	0.613
Maximum Void Ratio e_{max}	1.014
Permeability at e=0.72	0.98e-04 m/s
Angle of shearing resistance at critical state	32° (estimated value)

EXPERIMENTAL RESULTS

Visual Observations

Circular Tunnels

Visual observations revealed that the circular tunnels experience almost no deformation up to accelerations of 0.50g. A strong ovaling motion of the tunnel section was observed in the test series SUC-01 for the accelerations bigger than 0.50g. There has been an accumulation of the plastic strains in the flexible tunnel lining and finally the tunnel collapsed completely in test 7. The tunnel was squeezed and then closed in the horizontal direction. Active and passive wedges were observed to be formed as shown in figure 3.

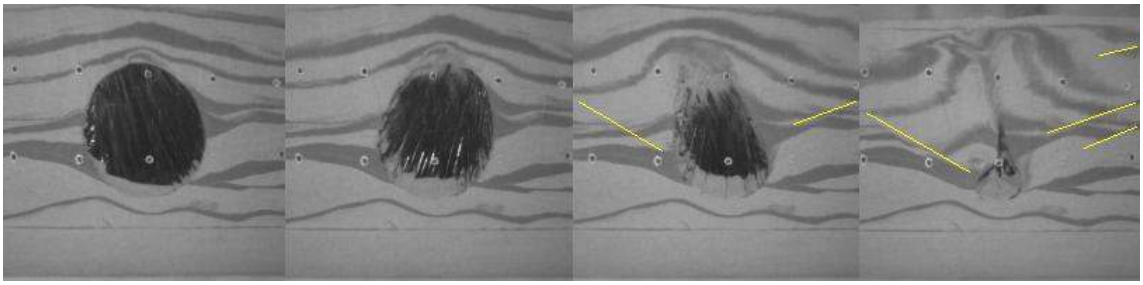

Figure 3. Progressive failure of the circular tunnel. Lines show the failure surfaces.

In test SUC-03, where an overburden pressure of 2.45 kPa was applied on the soil surface, the tunnel section didn't exhibit big ovaling motions and the collapse didn't occur.

Square Tunnels

Square tunnels didn't experience big deformations at accelerations smaller than 0.79g. Racking deformation observed at each cycle. But, the most drastic deformation was observed in the sidewalls of the rectangular tunnel section, where the soil next to the side walls was contributing to the deformation as the tunnel collapses by caving in as shown in figure 4.

Surface waves traveling on the soil surface were also captured. It was observed that the surface waves hit on top of the tunnel structure as they travel from one end towards the other end of the rigid box and cause sand particles to fly in the air.

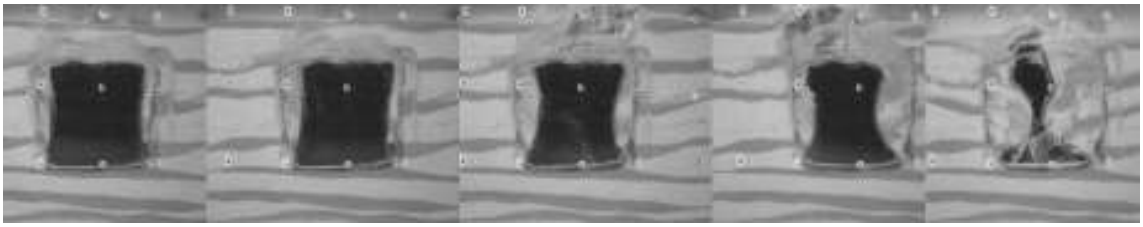

Figure 4. Progressive failure of the square tunnel.

In case of 2.45 kPa of overburden pressure applied on the soil surface, no big deformations were observed as a result of shaking and the collapse didn't occur.

Acceleration fields around the Tunnel

A comparison of the acceleration values in the free-field and around the tunnel revealed that the accelerations above the tunnel were higher than the accelerations recorded in the free field at the same depth for the tests without applied overburden pressure (SUC-01 and SUC-02). On the other hand, the accelerations at the bottom of the tunnel sections were smaller than the accelerations in the free field. This may be attributed to the fact that the flexible tunnel structure experiences more shear deformation compared to the soil in the free-field. Cumulative energy of the acceleration signals can be represented as Arias Intensity plots as shown in figures 5 and 6. Arias intensity is defined as (Arias, 1970):

$$I_a = \frac{\pi}{2g}\int_0^{\infty} a(t)^2\,dt \tag{5}$$

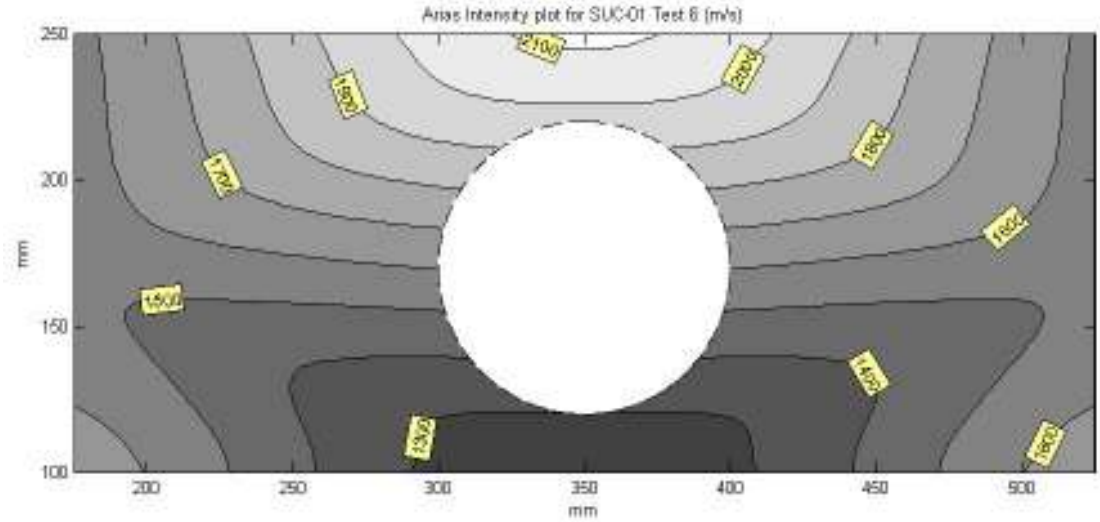

Figure 5. Arias Intensity plot for SUC-01 Test 6

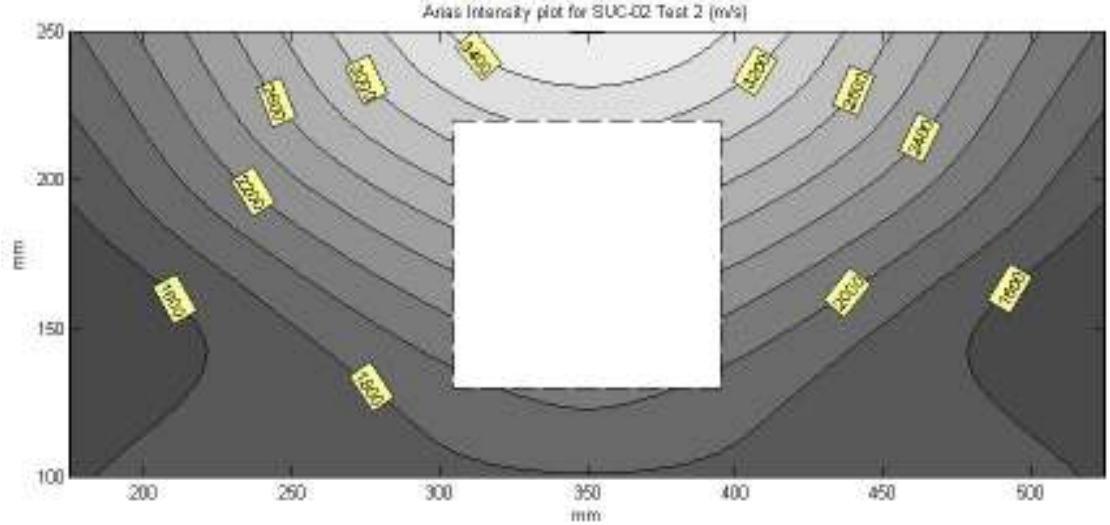

Figure 6. Arias Intensity plot for SUC-02 Test 2

For the test series SUC-03 and SUC-04 the accelerations in the middle of the sand bed were greater than the accelerations on the bottom and near the top of the sand bed. This may be due to a suppressed mode shape resulting from the weight of the heavy concrete block on top of the soil bed. Further investigation is needed to measure the amount of amplification between these accelerometers.

PIV Analysis

A quarter-cycle PIV analysis was conducted similar to the work by Knappett et al. (2005). The results show that the behavior tunnel-soil system varies between quarter-cycles of the sinusoidal input motion. The results presented below are for test SUC-01 Test 7. The sign convention used for the analysis is shown in figure 7.

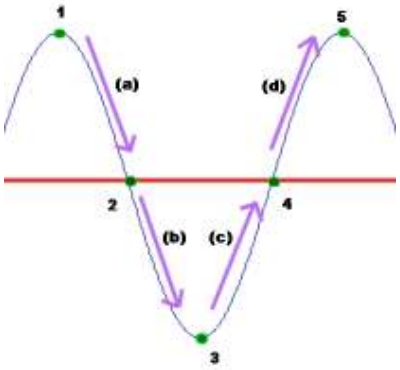

Figure 7. Sign convention for the quarter-cycle analysis

The quarter-cycle PIV analyses for the beginning and the end of earthquake is shown in figures 8 and 9. The rigid body movement of the container is extracted from the total movement of the sand patches. At location 1 the acceleration is maximum and the velocity is minimum. The box is at the right hand side. Figure 8a shows the relative soil movement while the box moves from location 1 towards left. The acceleration, which acts in the reverse direction, is decreasing towards zero whereas the velocity becomes maximum in this phase of the movement. The relative displacement of the sand particles is minimum. At the end of the second quarter-cycle (b) the acceleration is maximum and is acting in the opposite direction of the displacement. Although the rigid body moves towards right, the inertia of the sand particles, which are still trying to move towards left, causes a shearing to occur on the top of the soil bed. This is manifested by formation of the active and passive wedges next to the tunnel structure.

The flexible circular tunnel has collapsed 2.5 seconds after the shaking has begun. The sides of the tunnel closed horizontally due to accumulated strain throughout the cycles. At the beginning of the earthquake the tunnel section did the ovaling motion and then the aperture starts to get smaller and smaller while active and passive wedges start to form next to the tunnel. Since the tunnel liner is loaded beyond its elastic limit irrecoverable plastic strains occurred which lead to the collapse of the tunnel section. The resulting failure planes have angles of 20 to 26 degrees to the horizontal.
The shaking continued after the collapse. The quarter-cycle PIV analysis at the end of the shaking is shown in figure 9. PIV analyses show that the volume of the soil contributing to the active-passive wedge formation increased considerably.

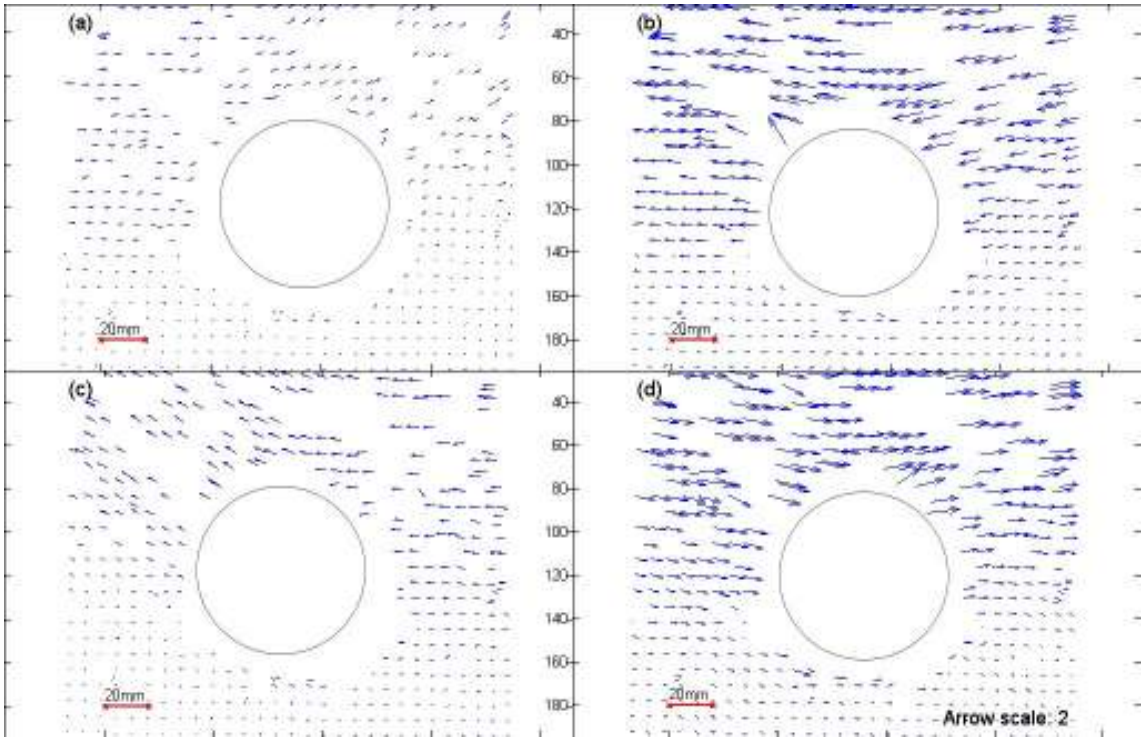

Figure 8. Relative movement of the sand with respect to the tunnel in a cycle at the beginning of the earthquake. Note that the circle is drawn to show the approximate location of the tunnel section. It is not to scale. Arrow magnification scale is 2.

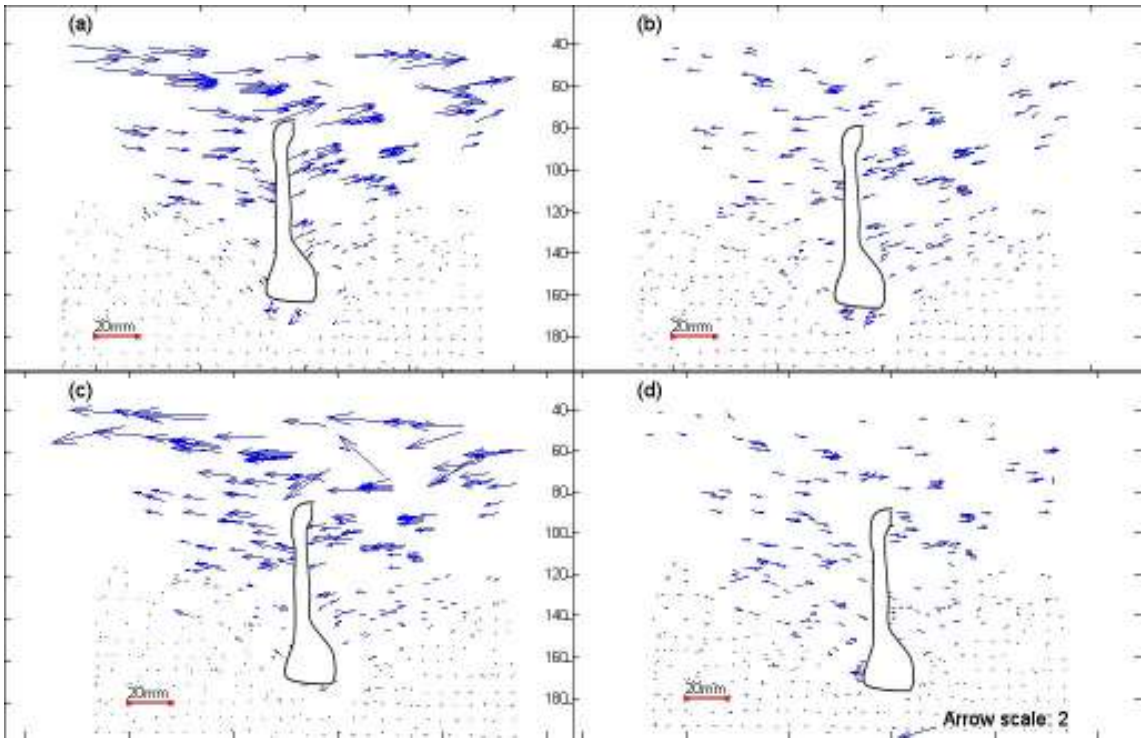

Figure 9. Relative movement of the sand with respect to the tunnel in a cycle towards the end of the earthquake. Note that the tunnel lining is not in its real shape. It is drawn to show the approximate location and the approximate shape after collapse. Arrow magnification scale is 2.

DISCUSSION

The shaking table experiments showed that the soil-structure interaction between the tunnel and the surrounding soil is strong. Tunnel section seems to collapse under strong shaking when there is no overburden pressure; typically for accelerations bigger than 1.2 g in this set of experiments. Collapse mechanism observed both visually and from PIV analyses suggests that the side walls are "caving in" and closing the tunnel. This suggests that at these locations the horizontal stresses are becoming larger than the vertical stresses. This may be due to the rigid boundaries which cause P-waves to be generated which are quite strong relative to the overburden stresses.

It was observed that active and passive wedges form during collapse of the tunnels. This type of mechanism, although needs further verification, may be plausible in case of shallow tunnels. This result suggests that the use of dynamic earth pressure methods for these cases may be a good approach. Acceleration fields observed around tunnels suggest that there is significant variation around the tunnel. The accelerations observed in the free-field are different than those around the flexible tunnel structure.

A significant difference has been observed between the soil-structure interaction behaviors of circular and rectangular tunnels. In case of rectangular tunnels, the top and the invert of the tunnel act like struts resisting lateral load but the flexible side walls collapse by caving in towards the tunnel cavity. The soil mass contributing to the deformation of the sidewalls is big as shown. The racking motion seems to make a smaller contribution to the plastic strains compared to the ovaling motion observed in circular tunnels. In case of circular tunnels, the ovaling of the circular cavity results in accumulation of plastic strains in each cycle. The tunnel cavity takes first an ellipsoid shape and then collapses.
It was observed that the tunnels deform less as the confinement increases. The free field shear deformations seem to be smaller when the overburden pressure increases.

It should be noted that the shaking table tests have limitations. First of all, the correct similitude can never be achieved as stated by Muir-Wood (2004). Secondly, the boundary effects are strong when the rigid boxes are used. Therefore the correct field conditions can never be obtained.

CONCLUSION

Current research methods are not satisfactory to explain the behavior of the underground structures subjected to earthquake loading. Analytical methods are based on elasticity theories and do not account for inertial effects. The numerical methods are complex and they still need to be verified using experimental data.

Small scale shaking table tests conducted on flexible tunnels in soft soil conditions showed that there is a strong soil-structure interaction between the tunnel and the surrounding soil, especially in case of shallow tunnels. The acceleration data suggest that there is variation of accelerations around the tunnel structure indicating a clean soil-structure interaction effect. Tests suggest that rectangular and circular tunnels behave different during earthquake. In case of rectangular tunnels, side walls seem to be quite critical for the overall stability of the tunnel section. The top and the invert of the rectangular section behave like struts, which support the sidewalls. The collapse occurs as a result of "caving-in" deformation of the side wall. The soil next to the side walls is contributing to the deformation more than it does in case of circular tunnels. Circular tunnels, on the other hand, collapse as a result of the accumulation of plastic ovaling deformation in each cycle. In both cases, active and passive wedges formed on either side of the tunnel section. This shows that dynamic earth pressure methods suggested in the literature may be useful for the dynamic analysis of shallow tunnels. It is also observed that tunnels subjected to high confinement stresses are more resistant to the earthquake motions.

Finally, it must be pointed out that further analyses using dynamic centrifuge testing are needed due to the low stress level at which the shaking table tests reported herein were carried out.

AKNOWLEDGEMENTS

The first author is grateful for the financial support provided by Yuksel Proje Uluslararasi A.S.

REFERENCES

Arias, A. "A Measure of Earthquake Intensity", Seismic Design for Nuclear Power Plants, MIT Press, Cambridge, Massachusetts, pp.438-483, 1970

Bobet A, Fernández G, Ramirez J, Huo H. "A Practical Method for Assessment of Seismic-Induced Deformations of Underground Structures", Proceedings of GeoCongress, Atlanta, USA, 2006

Esmaeili M, Vahdani S, and Noorzad A. "Dynamic response of lined circular tunnel to plane harmonic waves", Tunneling and Underground Space Technology, 21:511–519, 2006

Hardin BO and Drnevich VP. "Shear modulus and damping in soils: design equations and curves", Journal of the Soil Mechanics and Foundations Division, ASCE, 98, No.SM7, 667-692, 1972

Hashash YMA, Hook JJ, Schmidt B and Yao J I-Chiang. "Seismic design and analysis of underground structures", Tunneling and Underground Space Technology, 16:247–293, 2001

Huo H, Bobet A, Fernández G, Ramirez J. "Load Transfer Mechanisms between Underground Structure and Surrounding Ground: Evaluation of the Failure of the Daikai Station", J. Geotech. and Geoenvir. Engrg., Volume 131, Issue 12, pp. 1522-1533, 2005

Knappett JA, Haigh SK, and Madabhushi SPG. "Mechanisms of failure for shallow foundations under earthquake loading", Soil Dynamics and Earthquake Engineering, 2005

Marketos G, Madabhushi SPG. "An investigation of the failure mechanism of a cantilever retaining wall under earthquake loading", International Journal of Physical Modeling in Geotechnics, Vol.4, pp.33-44, 2004

Merritt JL, Monsees JE, and Hendron AJ. "Seismic design of underground structures", In Proceedings of the 1985 Rapid Excavation Tunneling Conference, volume 1, pages 104-131, 1985

Muir-Wood, D. "Geotechnical Modeling", Spon Press, 2004

Pakbaz MC and Yareevand A. "2-d analysis of circular tunnel against earthquake loading", Tunneling and Underground Space Technology, 20:411–417, 2005

Penzien J. "Seismically induced racking of tunnel linings", Earthquake Engineering and Structural Dynamics, 29:683 – 691, 2000

Penzien J and Wu CL. "Stresses in linings of bored tunnels", Earthquake Engineering and Structural Dynamics, 27:283 – 300, 1998

St.John CM and Zahrah TF. "Aseismic design of underground structures", Tunneling and Underground Space Technology, 2(2):165–197, 1987

Wang JN. "Seismic Design of Tunnels: A State-of-the-Art Approach", Monograph. Parsons,

Brinckerhoff, Quade and Dougless Inc., New York, 1993

Wang WL, Wang TT, Su JJ, Lin CH, Seng CR, Huang TH. “Assessment of damage in mountain tunnels due to the Taiwan Chi-Chi earthquake”, Tunneling and Underground Space Technology, 16:133–150, 2001

White DJ. “GeoPIV: Particle Image Velocimetry (PIV) software for use in geotechnical testing”, University of Cambridge Department of Engineering, Technical Report, pages CUED/D–SOILS/TR322, 2002